Bézier Curves-Based Novel Out-of-Path Beamforming Calibration Technique in IEEE 802.11 WLAN Networks

Mehdi Guessous, Lahbib Zenkouar

Abstract – *Beamforming is a major building block of Radio Resource Management (RRM) in WLAN networks that helps mitigate the interference and maximize the transmission opportunity of Access Points (AP) toward Wireless Devices (WD). In contrast to the related-work In-Path approaches, we propose a novel Out-Of-Path approach to beamforming calibration that is based on concepts from Computer Aided Graphical Design (CAGD) field and now-a-day network design best practices. The enhancement that the presented solution adds to the beamforming operation time and results' accuracy is investigated. It is demonstrated that the processing of beamformer's parameters: array elements' signal weighting and phase shifting, to achieve the desired angle of radiation, direction of arrival and gain, is possible at Wireless Lan Controller (WLC) level in indoor controlled WLAN networks. Further, we introduce in the same context, the concept of a pseudoAP, a virtual AP that represents a cluster of all possible real AP beamformers to a given WD and investigate the enhancement that it may add. The results of both simulations show an important enhancement of the conventional beamformer processing time at AP level. But at WLC level, a trade-off exists between maximizing the transmission opportunity and reducing the required processing time. Copyright © 2019 The Authors.*
Published by Praise Worthy Prize S.r.l. This article is open access published under the CC BY-NC-ND license (http://creativecommons.org/licenses/by-nc-nd/3.0/).

Keywords: *Beamforming, Bézier curves, Radio Resource Management, Signal Processing, Wireless Local Area Network*

I. Introduction

In the context of indoor controlled WLAN networks, designers and engineers deal with co-channel interference as a major issue in providing clients with a high end-to-end performance standard. An important time is spent on site surveys: active and passive, and on WLC: radio planning, transmit power adjustment, channel assignment, and Quality of Service (QoS) configuration. Dynamic RRM is one of these important routines that a WLC runs to ensure a quick network-wide adaptation to radio environment changes and client application needs. Its operation is further augmented by a set of at-AP-level on-chip features such as beamforming. In this scheme, the beamformer confines the radiated energy, carrying the of-interest WD communication, to only the direction of communication as opposed to an omnidirectional operation. Consequently, this feature allows a lessened AP to WD communication exposure to interference from the neighboring APs and enhanced signal quality. From an array (of antennae) signal processing perspective, a conventional beamformer operation consists of three main building blocks: generation of the shifted signals, weighting of the corresponding magnitudes, and summing them up before radiation. However, how are shiftings and magnitudes processed? An important block is added to the operation of the previous beamformer to process these parameters:

calibration. The aim of calibration is to setup the beamformer initially, and guarantee that this beamforming is efficient in time. Beamforming calibration in the context of unified WIFI architectures is the focus of this work.

We propose a novel at-WLC-level Out-Of-Path method of beamforming calibration and demonstate its addition to the current conventional beamfoming operation. The presented solution does not rely on In-Path, beamformer and WD, feedbacks to setup and calibrate beamforming parameters but instead, on the evaluation of the environmental radio condition that is out-of-path, processed at WLC level and engblobing this communication.

In Section II, the related-work in-path approaches are discussed. In Section III, some WIFI unified architecture, array beamforming and radiation, radio coverage modelization, Bézier curves, concepts that are the theoretical foundation of this work are recalled. In Section IV, the problem is formally set. In Section V, the presented solution is described in detail and how it could enhance the conventional beamformer operation. In Section VI, the results of the simulations are discussed and evaluated. In the end, the work is concluded. This paper is an extension of work originally presented in 2018 9th IFIP International Conference on New Technologies, Mobility and Security (NTMS) [1].

II.   In-Path Beamforming Related Work

The majority of WLAN communicating systems: APs and WDs are equipped with omnidirectional antennae or a set of a limited number of unidirectional antennae to mimic an omnidirectional operation. Ease and cheapness of such implementations are some of the reasons before their wide use. However, in dense WLANs, they may burden heavily the whole network capacity because of noise and interference. Beamforming that consists of spatially concentrating the radiated energy or filtering unwanted signals becomes the solution of choice to the previous design limitations and requires a change in the physical structure of both APs and WDs. This enhancement enables the network with new capacities and support of rich applications.

II.1.   Beamformers Classification

In array signal processing, beamforming is achieved by modifying certain emitter or receiver parameters: array elements' phase shiftings, sub signals' magnitudes, or weights. In conventional, fixed or switched-beam beamformers, weights and phasings do not adapt automatically to radio environment as in their couterparts, adaptative beamformers. In [2], beamformers are classified as data independent, statistically optimum, adaptative or partially adaptative. Dolph-Chebyshev is an example of a data independent beamformer. Statistically optimum beamformers include: Multiple Sidelobe Canceller (MSCB), Reference Signal (RSB), Max Signal to Noise Ratio (SNRB), Lineary Constrained Minimum Variance (LCMVB) beamformers. Lean Mean Square (LMSB) and Recursive Least Squares (RLSB) are examples of adaptative algorithm beamformers.

II.2.   Beamformers Calibration

The general purpose of calibration is to find the adequate weights and shiftings that apply to a beamformer to reproduce with fidelity the desired signal. The possible beamforming calibration approaches are either by estimating the signal's Direction of Arrival (DOA), at reception, or upstream, at source, by working on feedbacks from a test receiver or the target itself. In MSC beamformers, the interference is estimated first, by using weighted auxiliary channels. Then it is deduced from the main channel to keep solely the desired signal.

This technique supposes that the desired signal direction is known, and that auxiliary channels do not convey it. Similarly, knowing the time intervals of presence and non-presence of the desired signal and the corresponding direction of arrival, weights and phasings, could be chosen such as to maximize Signal to Noise Ratio (SNR). Using a reference signal, which is sufficiently like the desired signal, is another technique. Beamformer's parameters are chosen to minimize the error between the beamformer's output and the reference signal. In this scheme, it is not necessary to know the desired signal direction. In LCVM, constraints are applied per direction so that the desired signals are passed with a specific gain and phase. The beamformer parameters are chosen in a way to minimize the output power. Some examples of applied constraints are: point in a coverage area, derivative and eigenvector. More details on these constraint-based techniques are in [2].

Near-Field (NF) and Far-Field (FF) beamforming calibration techniques were discussed in works [3], [4] and [5]. They are hardly feasible in the context of indoor WLAN networks, as they require the implementation of a dedicated test architecture in parallel to the production network. However, near-field calibration methods may simplify receivers design and operation, if they are integrated to RRM centralized management at WLC-level.

II.3.   Out-Of-Path Calibration Method

The previously cited related-work beamformers calibration techniques: DOA-based or NF-based, could be qualified as In-Path because they work on either of the emitter, receiver or the signal characteristics. In this work and in the context of WLC-based indoor dense WLAN networks, a novel Out-Of-Path method that allows a beamformer to process its parameters independently of the desired signal, emitter or receiver is presented. This processing is rather based on the environmental radio characteristics estimation at WLC-level. It is a part of our solution described in [6] concerning a NURBS based technique in processing transmit opportunity maps in WLAN networks. The formalism of our solution is based on Bézier curves concepts that are well known in Computer Aided Graphical Design (CAGD) field.

III.   Theoretical Background

In this section, unified WIFI architecture, beam-based modelization approach to radio coverage, conventional beamforming and Bézier curves as they pertain to this study are discussed.

III.1.   Unified WIFI Architecture

Standalone AP deployments do not scale with dense and frequently changing radio environments. It is necessary to centralize the whole intelligence and unify network radio resource planning. In a unified WIFI architecture, a WLC acts a repository of APs intelligence, a radio resource planner and network integrator. It helps a WLAN integrate with the other network parts: LAN, MAN, WAN and DCN and fulfill its commitment to the end-to-end application QoS and Security Service Level Agreement (SLA). In Fig. 1, an example of such architecture is presented. In general, a WLC gathers information from three sources: the wired interface towards the datacenter, the radio interface of each associated AP, and on-the-air AP to AP messages. Two market leading implementations of such WLCs are the

Cisco 8540 Wireless Controller and the Aruba 7280 Mobility Controller. The rest of the study focuses only on Cisco solution.
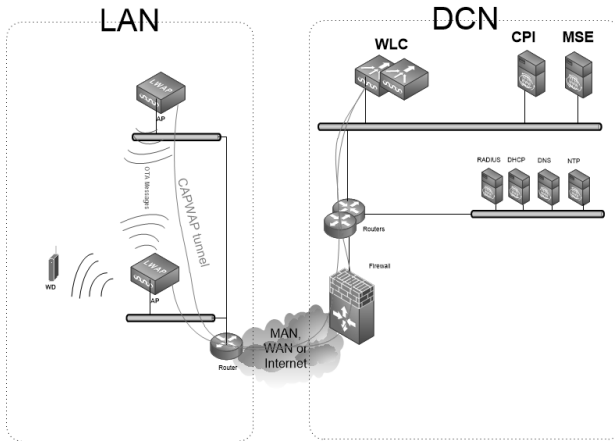

Fig. 1. An example of a WIFI architecture

Cisco unified WIFI architecture defines two protocols for the purpose of exchanging data between APs, and between APs and WLC:
- CAPWAP: stands for Control and Provisioning of Wireless Access Points and is used by APs to build a protocol association to the RF group leader WLC.
- NDP: is the Neighbor Discovery Protocol, it allows APs to send Over-The-Air (OTA) messages and exchange standard and some proprietary control and management information.

In addition to these protocols, Cisco APs embark a set of on-chip features: CLIENTLINK and CLEANAIR. The latter feature enables the APs to measure realtime radio characteristics and send them to the controller via the already established CAPWAP tunnels. Cisco appliances such as Cisco Prime Infrastructure (CPI) and Mobility Services Engine (MSE) may extend the capability of this feature to analytics on WIFI client presence, interferers management and heatmaps processing. CLIENTLINK in its 4.0 version, is the Cisco AP-level implementation of MU-MIMO IEEE 802.11ac beamforming. It works independently of CLEANAIR after the assessment of the quality of the channel. In this scheme, an AP sends a special sounding signal to all its associated WDs which report back their signal measurement. Based on these feedbacks, the AP decides on how much steering toward a specific WD is needed.

III.2. Beam-Based Modelization Approach to Radio Coverage

In a WLC-based network only a set of WDs: APs and certain WIFI clients with extended capability such as Cisco Connected Mobile Experience (CMX), can monitor coverage and report radio measures. Because it is not possible to monitor every area point, coverage modelization is necessary to predict these values at WLC-level. Based on the presumption that the measured

phenomenon is linear and on the enabled WDs' sporadic measures, we approximate the coverage of all the other points under the coverage area. In [7] and [8], two major modelization approaches families that may be referred to as "simplistic" and "idealistic" are discussed. In the first category, the coverage is approximated based on the range or distance of a WD from APs. In the second category, it is approximated based on the Voronoi or power diagram like zoning approaches. The first model divides a coverage area to three regions: transmission, interference or no-talk. The corresponding geometric pattern is a circle or disk and the interference at any point is approximated by the weighted intersection of all interferers' patterns. In the second model, the coverage area is rather segmented into non-uniform zones in the form of convex polygons. One particularity of this approach is that each zone corresponds to only and only one AP. Each zone's borderlines are defined based on the impact that neighboring APs may have on the zone's AP. In this "idealistic" scheme, co-channel interference is totally cancelled. The implementation of the "simplistic" approach is feasible and straightforward but have many limitations that burden its application: non-support of per-direction transmit power adjustment, coverage holes, non-support of obstacle detection, non-support of client localization, and non-detection of "hidden" transmit opportunities. The "idealistic" approach is the most performant, but it is not feasible: how is it costly possible to achieve any random polygon like propagation pattern?

In [7] and [8], a "realistic", beam-based, approach that is also, a generalization of the two previous ones is proposed. In this model, the covearge area of an AP is the area covered by the formed beams in each supported AP transmit direction. Not only transmit power level is tunable, direction can also be varied to achieve or approximate the desired performance. In Fig. 2, AP14 and AP15 "simplistic" coverage patterns, AP1 and AP2 "realistic' patterns and all APs "idealistic" patterns are shown. In Fig. 3, a compared model performance in a network of a random set of 30 APs in processing the coverage of a random set of 100 WDs is shown. In this simulation, APs support an equal number of 8 transmit directions, "R" represents the power level, "r" the sensitivity of a WD, "lambda" the attenuation of a signal from the source to the receiver in a free space condition, and "width" the beam aperture. In Fig. 4, it is shown that by decreasing the beam aperture and gain we could achieve an "idealistic"-like performance. Similarly, in Fig. 5, it is shown that by increasing beam "width" sufficiently we generalize our model to "simplistic"-like.

Further, implemented a per-AP power level adjustment "controlled" variant of the presented solution is presented, described in [8], and proved that it is comparable to a "Cisco"-like approach. In Fig. 6, we show an example of a test distribution of a random set of 30 APs and a random set of 100 WDs. Our RRM solution algorithm is tagged as "WLC2" whereas Cisco-like one is marked as "Cisco", "simplistic" as "Dir3" and "idealistic" as "Dir1".
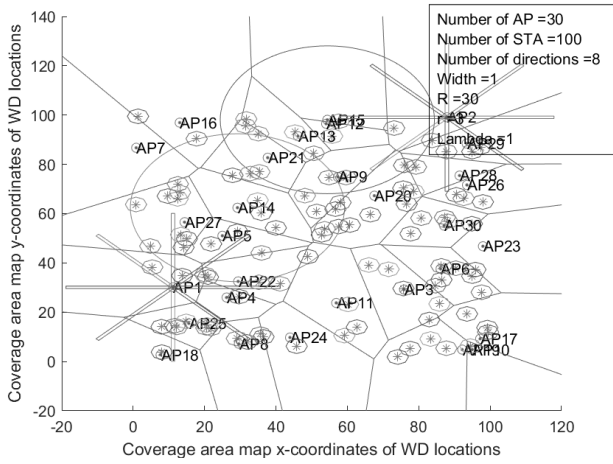
M. Guessous, L. Zenkouar
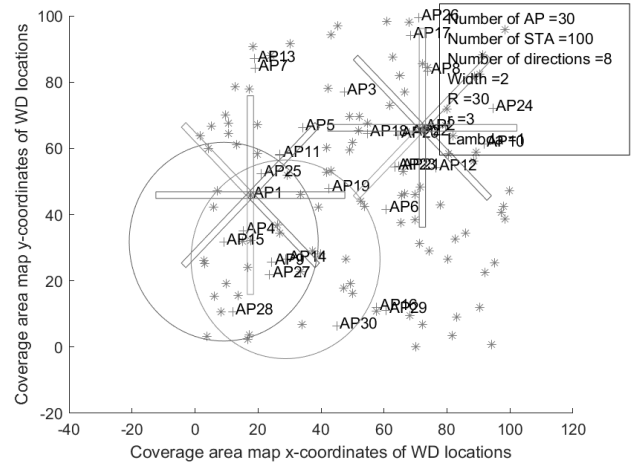

Fig. 2. Model coverge patterns

Fig. 6. Distribution example of 30 APs and 100 WDs
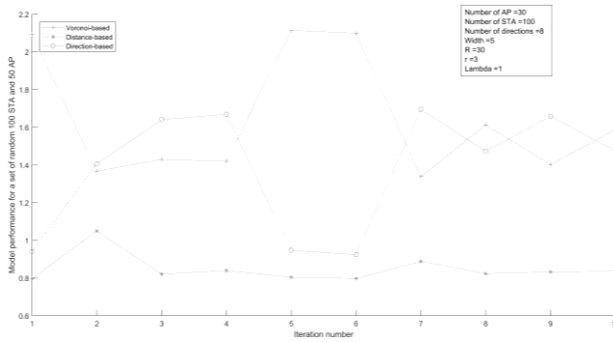
Fig. 3. Compared model performance

Fig. 4. Near "idealistic" model performance

Fig. 5. Near "simplistic" model performance

In Fig. 7, the corresponding "WLC2" transmit opportunity processing is shown.

In Fig. 8, the corresponding "Cisco" transmit opportunity processing is shown.

Fig. 7. "WLC2" opportunity processing example

Fig. 8. "Cisco" opportunity processing example

 Int. J. on Comp. and Comm. Netw., Comp. Intell. and Data Analytics, Vol. 3, N. 1

4

In order to enhance the results readability o, the variables names have been shortened in Table I.

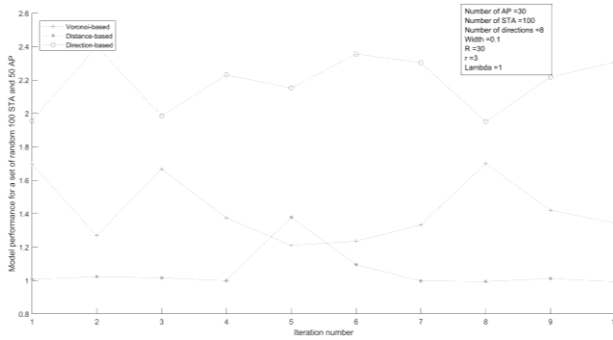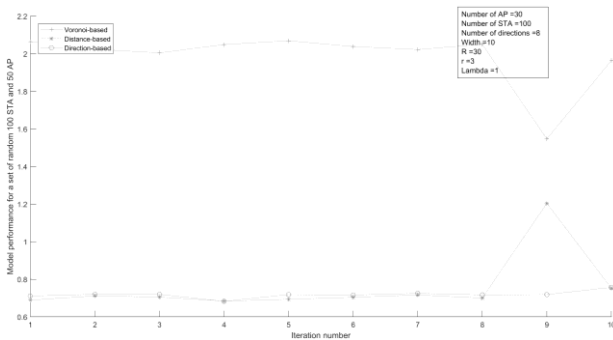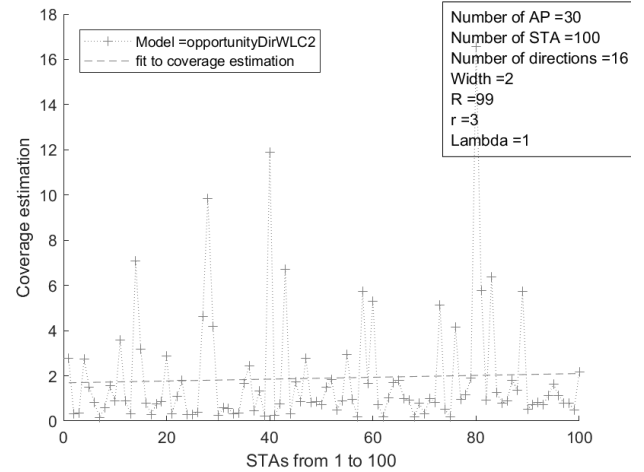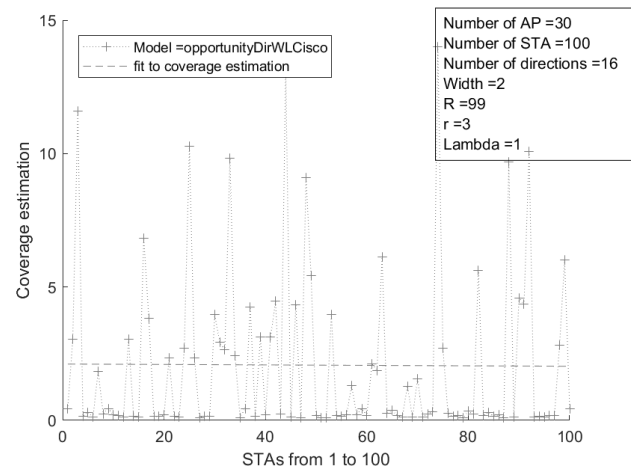| Variable old name	Variable new name
Mean Opportunity (in units)	M.O
Mean Interference (in units)	M.I
Dir. Optimal number	Dir.O
Detected Hole number	H.
Time (seconds)	T.

In Tables II, III, IV and V, the per model performance results of five iterations of the same simulation by choosing a random set of 30 APs and a random set of 100 WDs at each iteration are recorded. The "width" is equal to 0.1 unit value for "idealistic" model and to 10 unit value for the "simplistic". In general, it is obseerved that "WLC2" and "Cisco" model processing times are equivalent. Even if "Cisco" is more vulnerable to coverage holes, "WLC2" measured interference is higher in average. The "Cisco" model is the best performant if the measured transmit opportunity, interference, and coverage holes are considered equally.

TABLE II
"DIR3" BEAM-BASED MODEL PERFORMANCE RESULTS

Results	Simulation: iteration number AP=30, WD=100, Width=2, R=30, r=3, lambda=1				
	Itr=1	*2*	*3*	*4*	*5*
M.O	0.5	0.3	0.3	0.35	0.3
M.I	150	155	151	149	160
Dir.O	8	16	16	16	8
H.	0	0	0	0	1
T.	25.3856	25.1481	25.0731	25.0016	27.077

TABLE III
"WLC2" BEAM-BASED MODEL PERFORMANCE RESULTS

Results	Simulation: iteration number AP=30, WD=100, Width=2, R=30, r=3, lambda=1				
	Itr=1	*2*	*3*	*4*	*5*
M.O	0.5	0.8	0.4	1	0.5
M.I	40	52	64	60	45
Dir.O	8	16	16	16	8
H.	0	0	0	0	1
T.	82.566	169.5631	209.624	217.254	78.622

TABLE IV
"CISCO" BEAM-BASED MODEL PERFORMANCE RESULTS

Results	Simulation: iteration number AP=30, WD=100, Width=2, R=30, r=3, lambda=1				
	Itr=1	*2*	*3*	*4*	*5*
M.O	5	1	2.5	4	5
M.I	20	75	58	42	15
Dir.O	8	16	16	16	8
H.	5	0	0	3	8
T.	113.1636	179.8094	242.086	216.017	73.020

TABLE V
"DIR1" BEAM-BASED MODEL PERFORMANCE RESULTS

Results	Simulation: iteration number AP=30, WD=100, Width=2, R=30, r=3, lambda=1				
	Itr=1	*2*	*3*	*4*	*5*
M.O	2	1.4	1.5	1.4	1.35
M.I	1.5	1.6	1.5	1.4	1.75
Dir.O	8	16	16	16	8
H.	2	5	2	2	3
T.	26.5227	25.2914	25.0289	24.9015	26.132

For the rest of this work, it is considered that "WLC2" model is a "realistic" representation of a coverage area and that it could constitute a baseline for further optimization. In one hand, it was proven that "simplistic" and "idealistic" models are generalizable to beam-based equivalents: "Dir3" and "Dir1". In another hand, by setting adequately "width" value, optimizing the power levels and the number of supported transmit directions as it is described in [8], a comparable performance between "WLC2" optimized variant and "Cisco"-like implementation of RRM is observed over the same base coverage representation model: beam-based.

III.3. Classical Beamformer

In array signal processing, a general beamformer operation consists of generating sub-signals of the desired signal, phase siftings, magnitude weightings, summing the phase-shifted magnitude weighted sub-signals, and radiating the resultant signal. For the rest of our study, a simple form of such beamformer is considered: a linear array of *N+1* equidistant dipole antenna elements. If weights and shiftings are the same, then per the diffraction formalism, the wave intensity is a function of the resultant aperture θ, the distance between array elements d, and the phase shifting φ:

$$I = I_0 \left(\frac{\sin\left(\frac{\pi a}{\lambda} \sin\theta\right)}{\frac{\pi a}{\lambda} \sin\theta} \right)^2 \cdot \left(\frac{\sin\left(\frac{\pi N d}{\lambda} \sin\theta + \frac{N}{2}\varphi\right)}{\sin\left(\frac{\pi d}{\lambda} \sin\theta + \varphi\right)} \right)^2 \tag{1}$$

A further simplification of Formula (1), by taking $d=1/\lambda$, and maximizing the intensity, setting the second term numerator to *1*, is expressed by Formula (2):

$$\theta \approx \sin^{-1}\left(\frac{2}{N} - \frac{2\varphi}{\pi} \right) \tag{2}$$

III.4. Bézier Curves

Bézier curves are mainly known in the context of CAGD. The basic idea behind is to represent in a Cartesian plan any curve as a function of fixed points named definition or control points. Changing the allure of this curve is achieved by modifying the control points position, number or weights. In our context, control points represent the APs. Let P_0 be the AP of interest, AP_0, and at the same time the first and the last member in the list of control points, APs, that may have an impact on the transmit opportunity of AP_0 towards any WD. The region that hints on the impact of the neighboring APs over AP_0 to WD communication, is delimited by $B(t)$, the corresponding Bézier curve. This curve is expressed in Formula (3), as the sum of the control points in a new polynomial base defined by Bernstein polynomials:

Int. J. on Comp. and Comm. Netw., Comp. Intell. and Data Analytics, Vol. 3, N. 1

5

$$B(t) = \sum_{i=0}^{n} b_{i,n}(t) P_i , 0 \leq t \leq 1 \qquad (3)$$

In Formula (3), $b_{i,n}(t)$ is a Bernstein basis polynomial of degree n and P_i is a control point. An important property of Bézier curves, is that $P_0 P_1$ and $P_{n-1} P_0$ lines are tangent to the curve at P_0. This may hint on the transmit direction, beamformer's aperture, θ, that it is unlikely to be impacted by the neighboring APs. In Formula (4), θ is calculated that is a function of (x_1, y_1) and (x_{n-1}, y_{n-1}), the coordinates of points P_1 and P_{n-1}, respectively:

$$\theta = \sin^{-1} \frac{y_1}{\sqrt{x_1^2 + y_1^2}} - \sin^{-1} \frac{y_{n-1}}{\sqrt{x_{n-1}^2 + y_{n-1}^2}} \qquad (4)$$

In Fig. 9, AP_0 related Bézier curve is represented in a network of five neighboring APs. The formed lobe shape originating from AP_0 represents the impact (arrows from the APs toward the center of the lobe) that the neighboring APs have on any transmission AP_0 may have in the region.
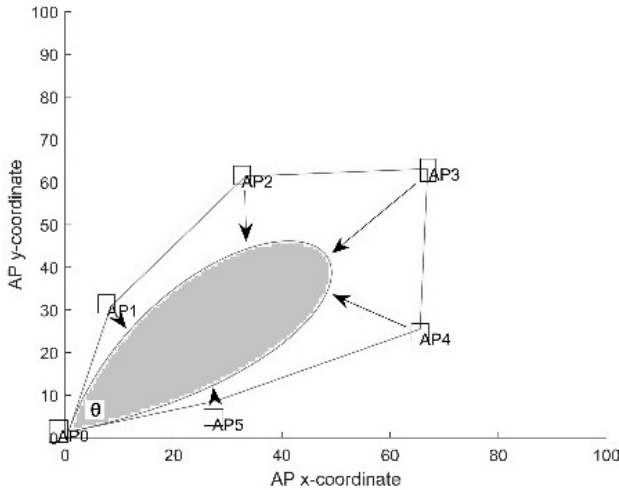

Fig. 9. AP0 derived radiation pattern

IV. Problem Description

This work does not focus on beamformers individual performance but rather on the enhancement, the presented solution may add to the general operation of a classical In-Path base beamformer in the context of indoor WLAN networks. In this preliminary work, we evaluate a beamformer two-step operation, which consists of the beamforming and adaptation functions, required processing time to achieve acceptable accuracy results.

Beamforming techniques have been categorized into: DOA-based and NF-based. In the first case, adaptation is triggered by the beamformer or target, whereas it is achieved at beamformer or source, in the second case model.

IV.1. DOA-Based Model

In this family of models and in the context of WLC-based indoor WLAN network, beamforming is adapted by comparing measured local signal characteristics at the receiver to the target ones. Based on interference and signal strength measurements from the receiver, WLC processes adaptation and apply it to the transmitter such as to maximize the radiation energy towards the target or beamformer. The necessary time for this adaptation is given by Formula (5):

$$T_{DOA} = T_{interference} + L \cdot (T_{eirp} + T_{proc} + T_{feed}) \quad (5)$$

In Formula (5), $T_{interference}$, is the necessary time for interference and local radio characteristics processing, L, the number of iterations to achieve the desired accuracy, T_{eirp}, the necessary time for signal strength measurement, T_{proc}, the necessary time for beamforming adaptation processing at WLC level, T_{feed}, the necessary time to report the measurements to the WLC. The interference processing depends on the chosen model, as it was described in [7] work and its extension [8]. In general, an area coverage representation model is either of Range-Based, or Zone-based. In these two cases the interference processing time is give in Formulae (6) and (7):

$$T_R = CONST + k(N - M) \cdot M \cdot T_{intersection} \qquad (6)$$

$$T_Z = CONST + k\big((M - 2) \cdot T_{iteration} + N \cdot T_{zone}\big) \quad (7)$$

In Formulae (6) and (7), k, the number of radio environment changes that may require a new coverage processing, is set to 1 for simplification. N and M are the control points, where coverage is processed, and the number of mobility devices: WDs and APs, respectively. $T_{intersection}$, is the required time to process an intersection between two transmit patterns in the coverage area. $T_{iteration}$, is the required time for an algorithm (Delaunay triangulation) iteration. T_{zone}, is the required time to locate a control point in a zone and deduce its corresponding transmit opportunity. In [6], the required interference time of the NURBS-optimized Beam-based representation of radio area coverage are processed as in Formula (8).

$$T_N = CONST + [M^2 - \left(1 - \frac{l}{z}\right)M + \frac{l}{z}M_{ineff}] \\ \cdot T_{surface} + [(k+1)(N - M)] \qquad (8) \\ \cdot T_{point}$$

In Formula (8), l, z and M_{ineff}, are the number of NURBS algorithm iterations (knots number calibration), the number of supported zones (for parallel processing) and the number of ineffective control points (M and M_{ineff} are subsets of N), respectively. η is a parameter that represents the scope of any change: minor, medium, or high. $T_{surface}$, is the time to process the coverage corresponding NURBS surface and T_{point}, the time to

process the corresponding value at any coverage point $P(x,y)$ in a 2D cartesian plan. In Formula (9), the following numerical simplifications are applied: $l=1$, $z=3$, and $\eta=0.25$. In fact, one iteration is sufficient for an acceptable accuracy, in most of the cases, in comparison with other algorithms and because the number of knots could be set to a higher level at algorithm initialization. $z=3$ is more to allow parallel processing when computing zones and may correspond to non-overlapping 3-channel coverage operation. $\eta=0.25$ supposes that most changes do not span multiple zones, that are confined to only one zone:

$$T_N = CONST + [M^2 - \frac{2}{3}M + \frac{1}{3}M_{ineff}] \cdot T_{surface}$$
$$+ [-\left(\frac{4+k}{4}\right)M + (\frac{4+k}{4})N] \qquad (9)$$
$$\cdot T_{point}$$

In this study, the maximum number of iterations L corresponds to the maximum number of the transmit directions that an AP supports in the worst case. It is also supposed that $T_{surface}$, $T_{intersection}$, T_{zone} and $T_{iteration}$ are equal and constant. T_{point}, is negligible in comparison with $T_{surface}$.

IV.2. NF-Based Model

In this family model, beamformer adaptation is processed by comparing the estimated distant signal characteristics at the transmitter to the target ones. In this scheme, no feedbacks are required from the receivers. WLC processes the adaptation and applies it to the transmitter to maximize the radiation energy towards the receiver. The necessary time for this adaptation is given by Formula (10):

$$T_{NF} = T_{interference} + L \cdot \left(T_{util} + T_{proc}\right) \qquad (10)$$

In Formula (10), the interference estimation time is equivalent to DOA-based family model. T_{util} corresponds to coverage representation model (Range-based, Zone-based or NURBS Beam-based) processing time of the transmit opportunity. The transmit opportunity represents the utile signal strenght to the interference and its processing time is equivalent to processing interference.

$$T_{util} \approx T_{interference} \qquad (11)$$

In [8], more details on this utility or opportunity processing are presented by model.

IV.3. Model Time Comparison

The necessary processing time per model (DOA and NF-based) and per coverage representation model (Range, Zone and NURBS-based), is a function of L, the number of iterations to achieve the desired beamforming accuracy, M, the number of mobility devices, N, the number of control points, and k, the number of radio environment changes. The NURBS based model's time, is in addition a function of M_{ineff} and l.

In Fig. 10, it is observed for low values of k, that Zone-based models time is better than the other models. For high N values, NURBS-based model time, with M_{ineff} equal to 10% of M, is dependent only on M, the number of control points.

All the other models show, in different proportion, that time is increasing with both M and N. In Fig. 11, for high k values, the NURBS-based model, with M_{ineff} equal to 10% of M, performance is equivalent to Zone-based "idealistic" model. Zone-based time is now dependent only on M whereas NURBS-based time is dependent on both. In Fig. 12, the maximum number of M is increased.

It can be observed that for high equivalent M and N numbers, both Zone and NURBS-based, with M_{ineff} equal to 10% of M, converge to the same time values.
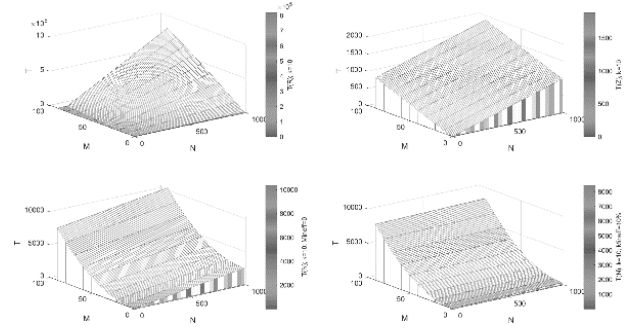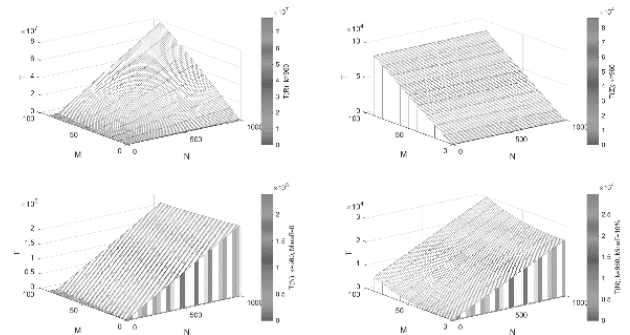

Fig. 10. Model time for low k values

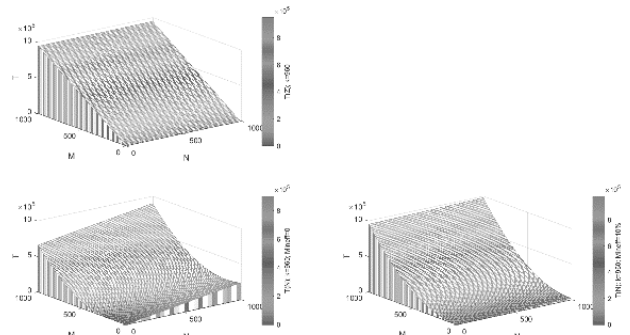

Fig. 11. Model time for high k values

Fig. 12. Model time for high equivalent N and M values

T_{NF} time is almost ($1+L$) higher than T_{DOA} time for each representation model: Range, Zone or NURBS-based. In the next section, we present and discuss our new Out-Of-Path approach to beamforming and the enhancement it may bring to the already discussed In-Path approach models, particularly to the NF-based beamforming at source model built on NURBS-enhanced Beam-based "realistic" representation of radio coverage area.

V. Out-Of-Path Beamforming Approach

In the context of WLC-based indoor WLAN networks, our solution processes beamforming adaptation by measuring the impact interferers may have over a certain transmission. Instead of processing the beamforming parameters from the signal at receiver or sender, such as in the In-Path approaches, the presented Out-Of-Path solution measures them directly, independently from the signal itself, by evaluating the impact interferences may have on the sender and receiver. A communication between an access point AP_0 and a wireless device WD_0 is considered. In a classical approach, WD_0 is associated with AP_0 and reports continuously the strength of the signal it measures from AP_0. Based on this signal measurement reporting, AP_0 decide on the necessary calibration to the beamformer operation to attain a maximum gain and consequent throughput toward WD_0.

In the presented approach, both AP_0 and WD_0 report their neighboring interferers (APs) to the WLC. The WLC evaluates the impact these interferers may have on AP_0 and WD_0 communication, by processing a special case Bézier curve that control points list includes AP_0 and the common interferences to both AP_0 and WD_0. One particularity of this curve is that it starts and ends at AP_0.and it is confined to the convex polygon described by the list of the control points. Another important property of this curve is that the segments defined by AP_0 and the second and before the last APs are tangent to AP_0 point. Knowing the shape of this curve, allows us to deduce immediately the beamforming shifting, for example, to apply. In Formula (12), φ, the necessary shifting, is expressed as a function of the second and before the last APs in the AP_0 control points' list:

$$\varphi \approx \frac{\pi}{2}\left[\frac{2}{N} - \sin\left(\begin{array}{c}\sin^{-1}\frac{y_1}{\sqrt{y_1^2+x_1^2}}-\\\sin^{-1}\frac{y_{n-1}}{\sqrt{y_{n-1}^2+x_{n-1}^2}}\end{array}\right)\right] \quad (12)$$

In the upcoming subsections, the solution workflow is detailed.

V.1. Processing of Control Points

The processing of control points is already included in the total processing of the coverage map of the NURBS-enhanced Beam-based representation model, more precisely in the processing of the NTO-CP algorithm detailed in [6]. The WLC processes for each WD, including APs, a list of interferers (neighboring APs) ordered by increasing signal strength, RSSI. These neighboring APs represent the control points that are used to draw the Bézier curves. Each control point weight matches the corresponding neighboring AP transmit power level inversely. A control point with a low weight pushes the curve perpendicular towards the AP to WD transmit direction axis; a high weight pulls the curve to the location of the point. The weighting of control points is achieved by adding the same control point many times to the list of knots. It is supposed that AP_1 has a power level of w_1, the lowest possible, and that AP_5 has a power level of w_5, the highest. Then, the list of the control points would include five occurrences of AP_1 and one occurrence of AP_5 to reflect the difference in power levels, or weights. We also expect that AP_5 is more distant from the curve than AP_1.

V.2. Processing of Beamforming Variables

As soon as the control points are identified for a given transmission (couple of an AP and WD), and at least three neighboring APs are detected, the processing of beamforming variables begins. First, the Bézier curve is drawn such as to start and end at AP_0, the AP of interest.

Second, we check that the area defined by this curve includes the WD of interest. If it is not the case, the control points weights are adjusted until this condition is satisfied. Third, we check that the area defined by the Bézier drawn curve is equivalent to any AP pattern in a given direction. If it is not the case, new control points are processed to achieve this condition. In Fig. 13, an example of a random distribution of 30 APs and 1 WD, and the corresponding Bézier curve, is shown. In this figure, the communication between WD_1 and the corresponding first (the highest RSSI), second and third APs: AP_7, AP_6 and AP_{15} is optimized. The resultant Bézier curve area includes the WD of interest, and then the first condition is satisfied.
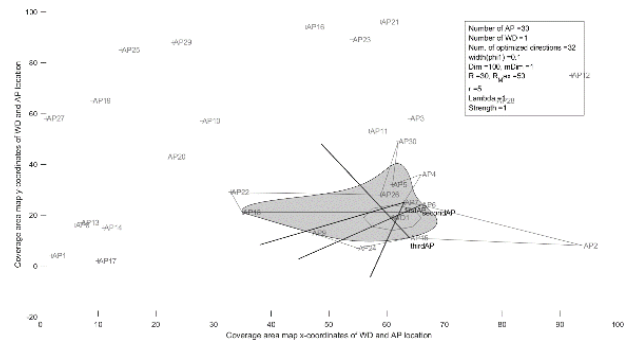

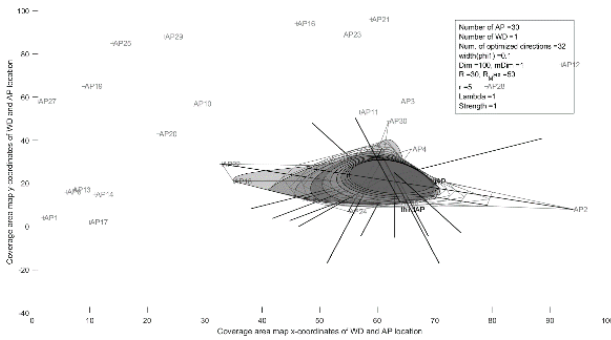Fig. 13. Bézier curve in a random distribution of 30 AP and 1 WD

In order to satisfy the second condition, we process new control points based on the initial set of control points. Each new control point is the baricenter of two consecutive old control points. In Fig. 14, we redraw the

 Int. J. on Comp. and Comm. Netw., Comp. Intell. and Data Analytics, Vol. 3, N. 1

8

corresponding Bézier curve several times until we get an acceptable precision. A more convenient alternative, than implementing literally the Formula (12), is to process the beamformer resultant aperture, by simply identifying the AP's direction that encompasses the maximum of the Bézier curve area.

V.3.   Total Processing Time

The new processing time, in Formula (13), corresponds to the required time to process the NURBS-enhanced Beam-based coverage interference plus the Bézier curve tuning time that is required to satisfy the second condition of our beamforming solution processing:

$$T_{NF,new} \approx (T_N - T_{CP}) + T_{CP} + L_2 \cdot T_{tuning} \qquad (13)$$

Fig. 14. Bézier curve area fitting

In Formula (13), T_{CP} is the time necessary to process the control points and is already included in T_N. L_2 is the necessary number of the Bézier curve redrawing iterations to attain the desired accuracy in beamforming processing results. T_{tuning} is the necessary time for one iteration. If T_{tuning} is neglected, in Formula (14), it can be stated that T_{NF} has enhanced theoretically. L is the number of iterations of the coverage processing; its maximum value is equal to the number of the supported directions per AP:

$$T_{NF,new} \approx \frac{1}{1+L} T_{NF} \qquad (14)$$

If the maximum number of the supported directions per AP is equal to eight directions, then the enhancement is almost 88.89% of the old processing time.

V.4.   Results Accuracy

The NURBS-enhanced Beam-based coverage representation model is adopted as the base of our evaluation of the beamforming operation accuracy of both NF-based and New NF-based models (NNF) or "BZ1" for further reference. For every WD we record the beamforming processing results, evaluate how similar are they, and compare the impact of NF-based and NNF-

based processings on the actual network to WD transmission. The ideal case is to have very similar beamforming processing results or quite different results with negligible impact on the transmission itself.

V.5.   Enhanced Beamforming Adaptation

In "BZ1", the AP decides to transmit towards a specific WD, and the WLC helps determine the beamformer parameters, thus the best performant direction. In this work, it is also investigated how the performance of our beamformer could be enhanced if we let the WLC decide also on the AP to handle the transmission and consequently the beamforming operation. In this scheme, marked as "BZ2" for further reference, we introduce the concept of a pseudoAP node to which a WD device is associated instead of the individual real AP. Each pseudoAP represents a cluster of real APs susceptible to handle the association of the same WD: first, second, and third RSSI strongest APs, as an example. The role of the WLC in this enhanced scheme, is to determine the best performant beamformer between the real APs and the corresponding transmit directions, in contrast with the first scheme.

VI.   Evaluation

This solution and the related-work approaches are evaluated in Matlab. Both approaches build on our "realistic" NURBS-enhanced Beam-based model representation of a WLC-based indoor WLAN radio coverage. In this preliminary work, we consider that the real condition measurements are between the "simplistic" and "idealistic" estimations. We believe that the results obtained by implementing the different approaches upon the same core base generalizable modelization realistic principles would lead to a comparable performance in a real implementation of the same approaches.

VI.1.   Test Methodology

At initialization, a random set of 30 APs are distributed on a 2D Cartesian plan such as in Fig. 13. The covered surface is only 100x100 meters, to simulate a highly dense network. Each AP supports a maximum of 32 transmit directions. For this simulation, we suppose that APs optimal transmit direction numbers converge to the same value. They support five transmit power levels, from 1 to 5, 5 being the highest. The WLC processes the optimum power level per AP; APs may have different transmit power levels. Level 3, the average, corresponds roughly to the recommended 67dBm signal at 30 meters from the AP. WD sensitivity is tuned to 10% of the maximum power level that an AP may support. L_2, the necessary number of the Bézier curve is set redrawing iterations to attain the desired accuracy in beamforming processing results, to a very large value, almost 20, and record the results for different large value sets of beam width and control point weight strengths. Width values

range in a logarithmic scale span from 0.1 (near "idealistic), 0.2, 0.5, …, 1, 2, 5, to 20 (near "simplistic").

Weight strengths values range is from 1 to 20. First, a power level and direction number optimized-coverage map, is processed. This step corresponds the to the processing of a NURBS-enhanced Beam-based radio coverage radio plan. Second, the WD's first, second and third AP are determined with the corresponding directions of association. At this stage, the NF-based beamformer has already processed the optimum beamforming direction. Third, the neighboring list of both the first AP and WD, is processed. Based on this list, the corresponding Bézier curve that represents the impact of the control points over the WD and its first AP is drawn L_2 time. We record the impact of the network on the first AP to WD communication each time. Fourth, the NNF-based beamformer optimum first AP direction is processed. In addition the impact that the network may have on second and third AP directions toward WD in a try to apply the pseudoAP enhancement is processed.

Last, the impact that the network may have on both the NF and last iteration NNF-based beamformers toward WD, communication is measured.

VI.2. Simulation Results of "BZ1"

In one simulation we vary the model "width", number of "tuning" iterations, and calibration weight's "strength", in the ranges defined in the previous subsection. In each iteration of this simulation we choose a new network of a random set of 30 APs. For one random WD, the first, second and third APs of association, related directions and network impact on each AP's transmission are recorded towards WD.

Similarly, "BZ1", the first variant of NNF-based model, results are recorded: the direction and corresponding network impact. For "BZ2", the second variant of NNF-based model, we record the new first AP of association, the related direction and network impact over a transmission towards WD. We evaluation "BZ1" results based on two criteria: the estimated interference deviance from NF-based model, that is our "truth", and the accuracy in having the predicted beamformer direction the same as the NF-based model processed direction. In Fig. 15, a density plot of the interference deviance "d_to_c" of an example of a 2226-record dataset is recorded. Most of the values are centered around zero which indicate that the estimated interference is equal to the "truth". In Fig. 16, a bar plot of the number of times the estimated direction corresponds to ± one direction to the direction of "truth" is shown. If "ap1bz1dir" is "True", then both the estimated and direction of "truth" correspond. The achieved accuracy of "BZ1", for all the dataset unfiltered, is almost 48.65% and corresponds to the count of "True" ratio to the total of counts which is 2226, the number of total records in this example simulation. For the subset of records that correspond to "width" = 0.1, the accuracy is only 21%. The accuracy for a "width" of

5, is higher and equal to almost 43.18%. For a "width" of 20, the accuracy is around 90.90%.
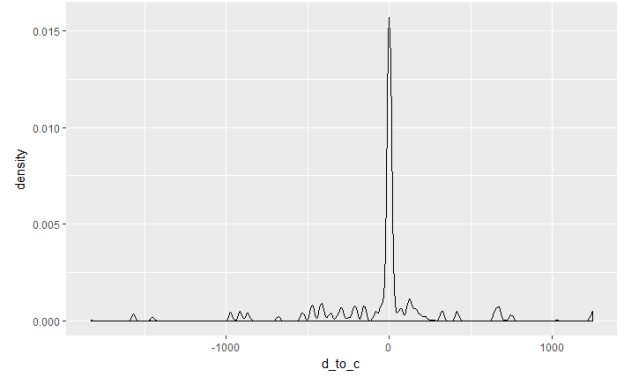

Fig. 15. Density plot of the interference deviance of an example of 2226-record simulation of "BZ1"
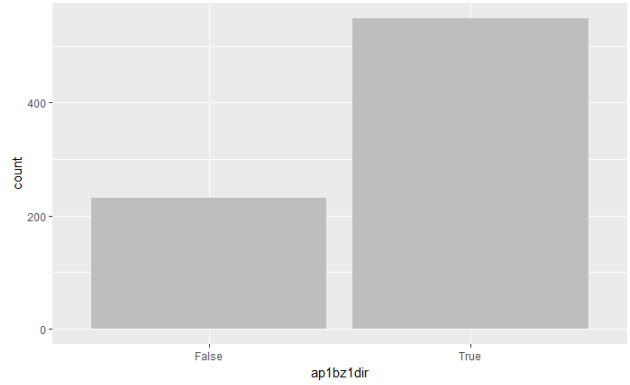

Fig. 16. Bar plot of the number of times the estimated direction corresponds to "truth" for "BZ1"

In Fig. 17, we exhibit that may exist between "d_to_c" and "width" is shown. It is important to note that most of "d_to_c" values are more concentrated around zero for "width" values in between 2 and 5 values. For "width" values more than 7, "d_to_c" values are sparse. In Fig. 17, "zone1" corresponds to the worst case, and "zone2" to the best.
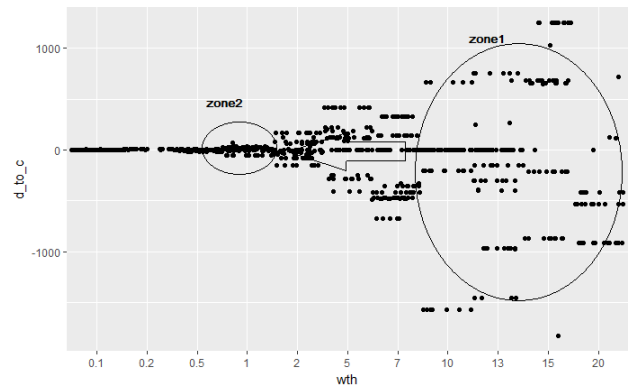

Fig. 17. Point plot of dataset "width" and "d_to_c" for "BZ1"

In Fig. 18, the relation that exists between "ap1bz1dir" and "width" is shown. We check that values of "True"

and "False" are comparable for "width" values less than 7. For "width" values more than 10, "False" counts are negligible in comparison with "True" count. As explained previously, more "d_to_c" is negligible and the accuracy is important, more NNF-based solution is time efficient in comparison with NF-based solution. Thus, for our example simulation, we check that by tuning "width" to a value around 2 and 5, we achieve an accuracy between 51.13% and 43.18%. The mean, *m*, and standard deviation, *s*, of "d_to_c" are equal to (1.43; 88.95) and (49.53; 223.73) for "width" values: 2 and 5 respectively. We check that by using "width" equal to 2, we enhance remarkably "d_to_c" results.
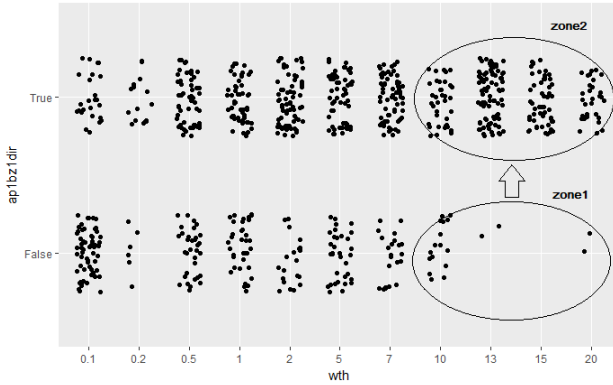
Fig. 18. Point plot of dataset "width" and "ap1bz1dir" for "BZ1"

Choosing a "width" value of 2, in the example simulation, may enhance NF-based processing time by roughly 51.13% of the theoretical value expressed in Formula. 14.

It should be noted that "c", the NF-based interference measurement of reference, (*m*; *s*)'s values are equal to (399.17; 567.25) and the (*m*; *s*) values of "d_to_c" are equal to (49.62; 381.82) for the whole dataset. In Fig. 19, the relation that may exist between "d_to_c" and "strenght" is investigated.

It can be noticed that "d_to_c" values converge to values tightly around zero when "strenght" increases. Starting from "strenght" value of 13, "d_to_c" values are less sparse around zero than 5 or 6 "d_to_c" values. In Fig. 19, "zone2" corresponds to the best case and "zone1" to the worst one.
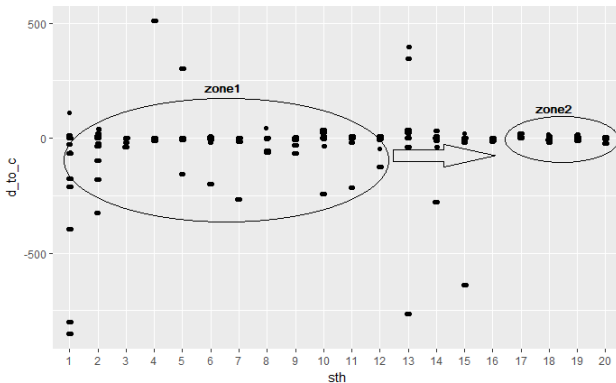

Fig. 19. Point plot of dataset "strenght" and "d_to_c" for "BZ1"

In Fig. 20, the relation that exists between "strength" and "ap1bz1dir" is shown. It is hardly to see a correlation in between the variables. However, we still notice that the zone around "strength" 1, 2 and 5 values is denser than for the highest "strength" values. From Fig. 19 and Fig. 20, it is noticed that increasing "strength" has a remarkable impact in decreasing "d_to_c" and a very slight effect on "ap1bz1dir": it is necessary to change "strength" from 1 to 16 values, to begin to see a difference. In Fig. 21, the relation between "tunings", L_2 curve tunings number, and "d_to_c" is shown. We notice that the majority of "d_to_c" values are around zero. The part to the left of this majority column has not changed.

However, in the right part and starting from the 12th tuning, values far from zero has lessened. In Fig. 21, "zone1" corresponds to the worst case.
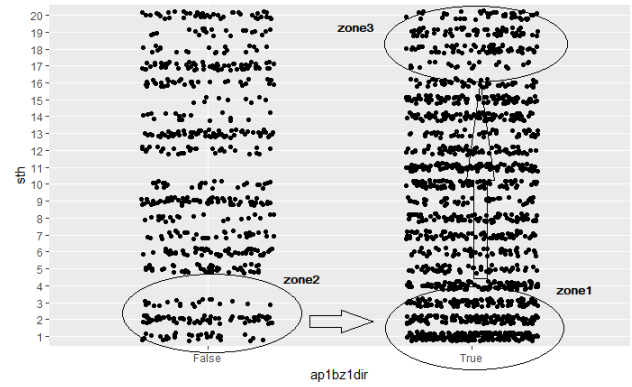

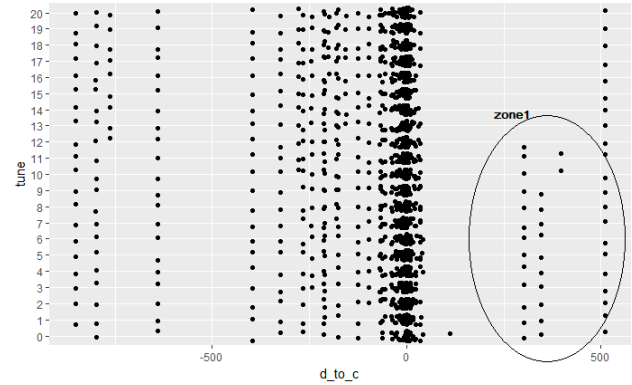Fig. 20. Point plot of dataset "strength" and "ap1bz1dir" for "BZ1"

Fig. 21. Point plot of dataset "tunings" and "d_to_c" for "BZ1"

In Fig. 22, the relation between "tuning" and "ap1bz1dir" is shown. In this plot, any dependency between the two variables is hardly observed.

In Fig. 21 and Fig. 22, it is observed that deepening tuning has enhanced the values of "d_to_c" but has no effect on "ap1bz1dir" even if the "tunings" range is extended to 20 times.

VI.3. Simulation Results of "BZ2"

In the second variant of our solution "BZ2" the situation is different as we offer the WLC the possibility

to choose the AP of association among the neighboring APs. In "BZ2" we evaluate only the "d2_to_c" estimate of the network impact on a random AP to WD communication deviance from "c" the NF-based model measurement, our "truth". In Fig. 23, the density plot of "d2_to_c" values is shown. The observed result is equivalent to "d_to_c".
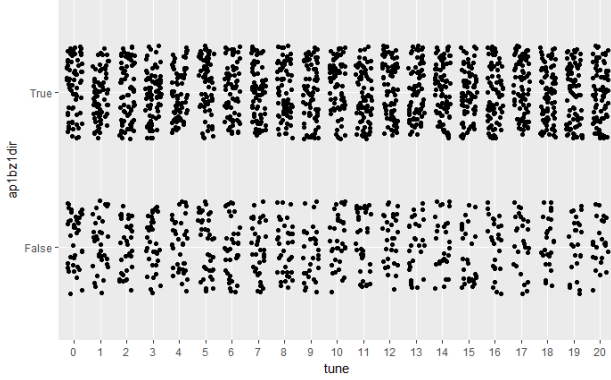

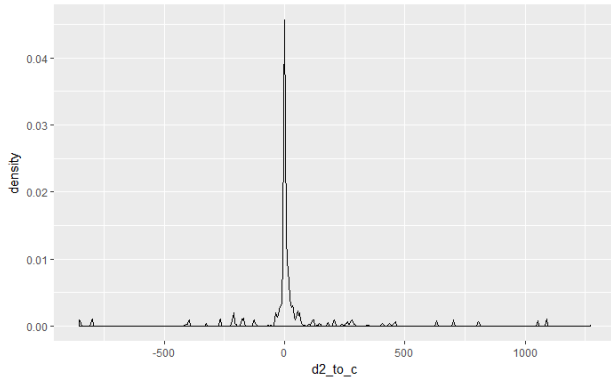Fig. 22. Point plot of dataset "tunings" and "ap1bz1dir" for "BZ1"

Fig. 23. Density plot of the interference deviance of an example of 2226-record simulation of "BZ2"

In Fig. 24, "ap1bz2ap" is plotted, and it shows the difference between the NF-based and the "BZ2" second variant NNF-based model processing of the first AP. We observe that NF-based and "BZ2" AP choices are remarkably different; "True" is only 14.64% of the total count. Differently from "BZ1", the previously calculated percentage does not affect the processing time of "BZ2" variant. The reason is that "BZ1" first AP processing, dependent on NF-based model, is no more considered the best choice. "BZ2" competes, independently from NF-based model, to propose the best first AP and beamformer. Consequently, "BZ2" achieves almost 100% enhancement of the theoretical NF-based model processing time expressed in Formula. 14. In Fig. 25, the relation between "d2_to_c" and "width" variables is investigated. Similarly to "BZ1", a remarkable gap of "d2_to_c" values is noticed when "width" is in between 2 and 5 values. "zone1" corresponds to the worst case and "zone2" to the best. In Fig. 26, "d2_to_c" and "strength" are plotted. Similarly to "BZ1", the same impact of increasing "strength" values can be noticed.
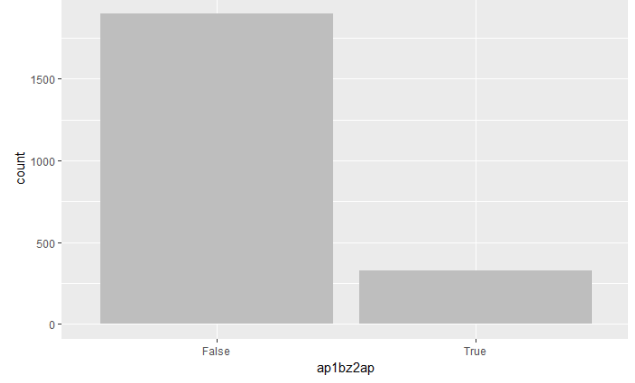

Fig. 24. Bar plot of the number of times the estimated direction corresponds to "truth" for "BZ2"

In Fig. 27, values of "d2_to_c" and "tunings" are plotted. It is noticed that deepening tuning tightens the base column values around zero when the tuning is at the 14th or 15th iteration.
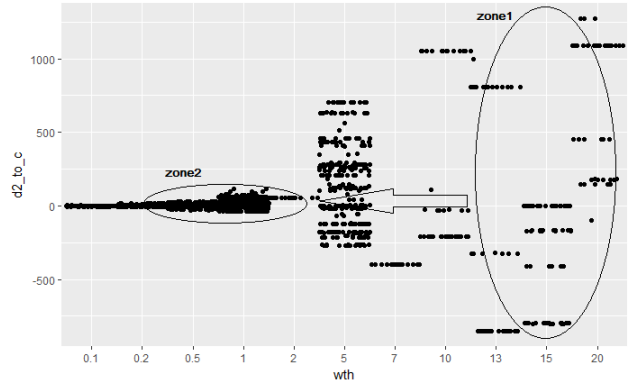

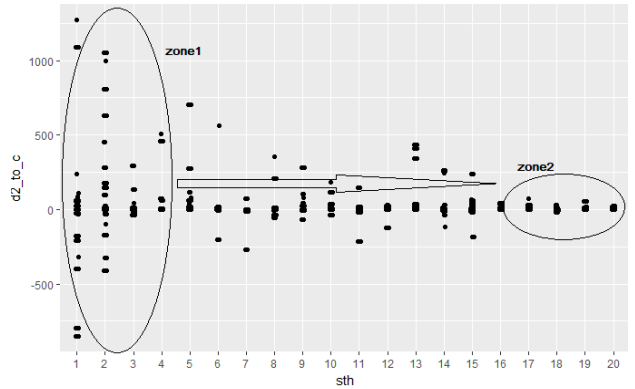Fig. 25. Point plot of dataset "width" and "d2_to_c" for "BZ2"

Fig. 26. Point plot of dataset "strength" and "d2_to_c" for "BZ2"

In order to evaluate "BZ2" we focus only on how far "d2", the "BZ2" estimated network impact on the AP to WD communication, is from "c", the NF-based model measured network impact on AP to WD communication, the "truth". For this example of simulation, "d2_to_c" mean is equal to 114.71 and it is higher than "d_to_c" mean: 49.62 units value. The standard deviation is 458.11 and 381.82 for "d2_to_c" and "d_to_c", respectively. In Fig. 28, the difference distribution

between "d_to_c" and "d2_to_c" is plotted. It is important to note that the majority of non-zero values, in "zone1", are recorded for the highest numbers of simulation iterations. These numbers correspond to the highest values of "width", "strength" and "tuning". They are outliers that may falsify our results.
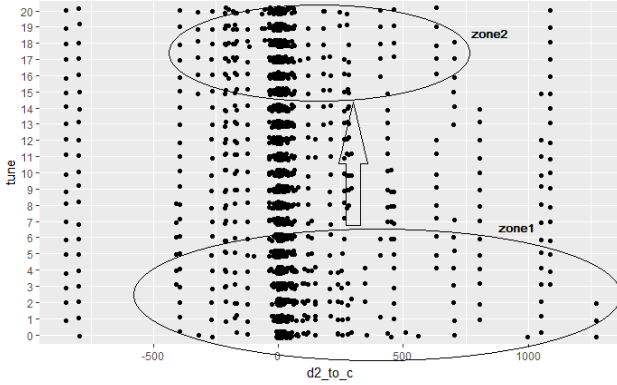

Fig. 27. Point plot of dataset "tunings" and "d2_to_c" for "BZ2"
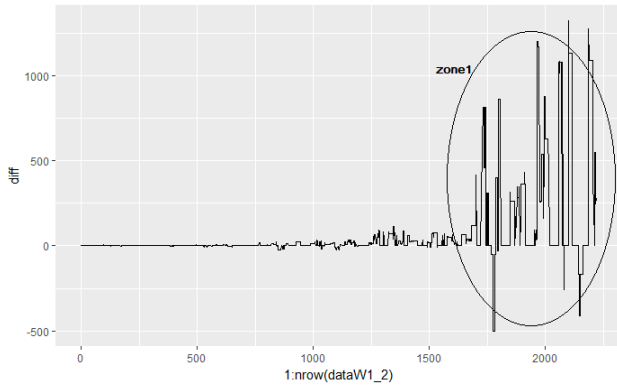

Fig. 28. Line plot of "d_to_c" and "d2_to_c"
difference "diff" per simulation iteration

VI.4. Results Generalization

In order to confirm the tendency of the presented results, the previous simulations are redone for the same ranges of "width", "strength" and "tunings", 5 times.

It should be noted that the number of one simulation iteration is equal to 4,400 iteration and corresponds to the "width" range size multiplied by the "strength" range size multiplied by the "tunings" range size. The maximum total number of records is equal to 22,000 records. In each iteration, a random distribution of 30 APs and one WD is generated. All APs distributions that do not provide WD with at least three APs of association are ignored. For readability of our results variable names are corresponded to a shortened version in Table VI. In Tables VII and VIII, the results of the presented simulation iterations are shown. At each iteration, we record these variables: accuracies, means, standard deviations from means, best "width", "strength" and "tuning" value ranges. The remaining records are gathered by directly comparing the related plots similarly

to the ones presented in the last two subsections. Due to the available space in this article, not all the results are plotted. Only specific plots of a certain interest may be plotted.

TABLE VI
VARIABLES SHORTENED NAMES

Variable old name	Variable new name
"BZ1" Acc. ALL In %	BZ1.Ac
"BZ1" Acc. Width2 In %	BZ1.Ac2
"BZ1" Acc. Width5 In %	BZ1.Ac5
"c" mean	M.C
"BZ1" "d_to_c" mean	M.D-C
"BZ1" "d_to_c" mean Width2	M.D-C2
"BZ1" "d_to_c" mean Width5	M.D-C5
"BZ2" "d2_to_c" mean	M.D2-C
"BZ2" "d2_to_c" mean Width2	M.D2-C2
"BZ2" "d2_to_c" mean Width5	M.D2-C5
"c" Std. dev.	S.C
"BZ1" "d_to_c" std. dev.	S.D-C
"BZ1" "d_to_c" std. dev Width2	S.D-C2
"BZ1" "d_to_c" std. dev Width5	S.D-C5
"BZ2" "d2_to_c" std. dev.	S.D2-C
"BZ2" "d2_to_c" std. dev Width2	S.D2-C2
"BZ2" "d2_to_c" std. dev Width5	S.D2-C5
"BZ1" Best Width value range	BZ1.Wth
"BZ1" Best Strenght value range	BZ1.Sth
"BZ1" Best Tuning value range	BZ1.Ting
"BZ2" Best Width value range	BZ2.Wth
"BZ2" Best Strenght value range	BZ2.Sth
"BZ2" Best Tuning value range	BZ2.Ting
Difference between "d_to_c" and "d2_to_c" in %	D2-D

TABLE VII
"BZ1" SIMULATION ITERATIONS GENERAL RESULTS

Results	Simulation: iteration number, records count AP=30, WD=1, lambda=1				
	Sim.= (1,2226)	*Sim.= (2,3045)*	*Sim.= (3,2163)*	*Sim.= (4,2730)*	*Sim.= (5,3444)*
BZ1.Ac	55.79	52.97	49.97	54.87	53.10
BZ1.Ac2	100	53.55	47.61	71.42	42.85
BZ1.Ac5	72.38	67.34	94.70	56.90	61.37
M.C	131.38	306.82	193.66	308.04	377.21
M.D-C	42.06	29.88	21.22	10.12	33.00
M.D-C2	64.77	17.96	4.34	11.40	5.14
M.D-C5	102.13	92.45	245.23	22.79	75.72
S.C	311.92	562.33	375.67	792.57	675.94
S.D-C	163.26	226.78	378.40	442.90	305.96
S.D-C2	14.84	78.94	65.80	66.02	98.99
S.D-C5	282.62	264.29	301.99	375.57	395.67
BZ1.Wth	2	2	2	2	2
BZ1.Sth	15:17	15:17	12:13	15:20	16:19
BZ1.Ting	16	10:20	17:20	1:10	1:8

TABLE VIII
"BZ2" SIMULATION ITERATIONS GENERAL RESULTS

Results	Simulation: iteration number, records count AP=30, WD=1, lambda=1				
	Sim.= (1,2226)	*Sim.= (2,3045)*	*Sim.= (3,2163)*	*Sim.= (4,2730)*	*Sim.= (5,3444)*
M.C	131.38	306.82	193.66	308.04	377.21
M.D2-C	23.40	58.64	54.55	80.95	98.81
M.D2-C2	52.02	36.83	207.10	166.32	78.32
M.D2-C5	125.16	123.00	5.31	175.53	98.12
S.C	311.92	562.33	375.67	792.57	675.94
S.D2-C	227.91	347.56	352.72	355.26	371.18
S.D2-C2	0	100.16	94.64	78.85	101.56
S.D2-C5	273.89	697.16	223.72	390.01	417.88
BZ2.Wth	0.1:2	0.1:2	0.1:2	0.1:2	0.1:1
BZ2.Sth	16:20	15:20	13:20	14:20	15:20
BZ2.Ting	14:20	16:20	8:20	7:20	10:17

In Table IX, we record the percentage of significant differences in processing the "d" and "d2" network impact on beamforming operation. The lower this percentage is, the better is the match between "BZ1" and "BZ2". In this simulation, a 35.54% average difference is achieved.

TABLE IX
"BZ1" AND "BZ2" DIFFERENCE
SIMULATION ITERATIONS GENERAL RESULTS

Results	Simulation: iteration (number, record count) AP=30, WD=1, lambda=1				
	Sim.= (1,2226)	*Sim.= (2,3045)*	*Sim.= (3,2163)*	*Sim.= (4,2730)*	*Sim.= (5,3444)*
D2-D	23.62	27.75	30.65	45.05	50.63

In general, that the results tendency is confirmed when varying "width", "strength" and "tunings", is remarkably the same as it was presented in the last two subsections which leads to these important conclusions:
- accuracy of "BZ1" is almost 53.34% average,
- "do_to_c" and "d2_to_c" means of both "BZ1" and "BZ2" are significantly less than NF-based ones,
- "do_to_c" and "d2_to_c" standard deviations of both "BZ1" and "BZ2" are equivalent to NF-based ones,
- "width" value 2, represents the best tradeoff between minimized "d" deviation from "c" and direction matches, in "BZ1". It allows the best performance in "BZ2", too.
- the best "strength" values for "BZ1" and "BZ2" are, in average, in 14:17 and 14:20 ranges, respectively.
- the best "tunings" values for "BZ1" and "BZ2" are, in average, in 9:15 and 11:19 ranges, respectively.
- the difference between "d_to_c" and "d2_to_c" measures, is negligible for the first 64.45% average of the iterations range values.

VII. Conclusion

In this work, a novel Out-Of-Path calibration technique of beamformer, at source, in the context of indoor dense WLAN networks has been presented. The approach is based on concepts from CAGD in measuring the impact the network may have on a specific communication.

Two variants of the solution have been presented: "BZ1" and "BZ2". It has been observed that both implementations' deviation from "truth", NF-based measured network impact on beamformer to beamformer communication, are comparable.

In the first case, "BZ1", an average of 53.34% accuracy is achieved, that is reflected directly on the necessary time to process NF-based approach beamforming. In the second case, "BZ2", the accuracy measurement is not relevant. Only the deviation from the "truth" measurements indicates the performance of our solution and we achieve a 100% of the theoretical processing time in comparison with the NF-based model approach. We observed that the difference between "BZ1" and "BZ2" measurements is very negligible for

the first 64.45% iteration records. By tuning model variables: "width", "strength" or "tuning", we could achieve even better results.

In the context of indoor dense WLAN networks, it is necessary to help APs decide on beamforming parameters because they do not have an overview of the network condition as a WLC may have. Our work enhances the efficiency of this operation by checking first the feasibility of the operation. This is to prevent wasting time on calibrating beamformer parameters when the network is heavily impacted by interference and offering no possibility for the operation to succeed. Another advantage of our approach is to alleviate the processing time at AP level by reducing the circuitry and complexity of the current embarked adaptative beamformers.

Acknowledgements

References

[1] M. Guessous, L. Zenkouar, Bézier curves-based novel calibration technique of beamformers in IEEE 802.11 WLAN networks, 2018 *9th IFIP international Conference on New Technologies, Mobility and Security (NTMS),* pp. 1–5, Paris, April 2018.
https://doi.org/10.1109/NTMS.2018.8328682

[2] B. D. Veen, K. M. Buckley, Beamforming: a versatile approach to spatial filtering, Reflection properties of the Salisbury screen, *IEEE ASSP Magazine,* Volume 5, (Issue 2), April 1988, Pages 4–24.
https://doi.org/10.1109/53.665

[3] J. Lee, E. M. Ferren, D. P. Woollen, K. M. Lee, Near-field probe used as a diagnostic tool to locate defective elements in an array antenna, *IEEE Transactions on Antennas and Propagation,* Volume 36, June 1988, Pages 884–889.
https://doi.org/10.1109/8.1192

[4] M. Shafiee, S. Ozev, Contact-less near-field measurement of rf phased array antenna mismatches, *2017 22nd IEEE Test Symposium (ETS), pp. 1–6, Limassol, July 2017.*
https://doi.org/10.1109/ETS.2017.7968216

[5] J. P. Brandissou, P. Maes, E. Ongareau, J. C. Sillon, J. Wyrwinski, A 30 MHz-18 GHz fully automated far-field antenna measurement system, *1993 IEEE Instrumentation and Measurement Technology Conference,* pp. 178–182, Irvine, August 1993.
https://doi.org/10.1109/IMTC.1993.382656

[6] M. Guessous, L. Zenkouar, A NURBS Based Technique for an Optimized Transmit Opportunity Map Processing in WLAN Networks, *Lecture Notes in Computer Science*, vol 10372. Springer, Cham, 2017, pp. 143-154.
https://doi.org/10.1007/978-3-319-61382-6_12

[7] M. Guessous, L. Zenkouar, Cognitive directional cost-based transmit power control in IEEE 802.11 WLAN, *2017 International Conference on Information Networking (ICOIN),* pp. 281–287, Da Nang, January 2018.
https://doi.org/10.1109/ICOIN.2017.7899520

[8] M. Guessous, L. Zenkouar, A novel beamforming-based model of coverage and transmission costing in IEEE 802.11 WLAN networks, *Adv. Sci. Technol. Eng. Syst. J.,* Volume 2, (Issue 6), September 2017, Pages 28–39.
https://doi.org/10.25046/aj020604

Authors' information

Equipe de Recherche en Smart Communications – ERSC (ancien LEC), Centre de Recherche E3S, Département Génie Electrique, Ecole Mohammadia d'Ingénieurs – EMI, Mohammed Vth University in Rabat, Rabat, Morocco.

Mehdi Guessous was born in Fez, Morocco, on February 23, 1981. He received the degree of Engineer from Ecole Mohammadia d'Ingénieurs, Rabat, Morocco, in 2004 and the degree of Mastère Spécialisé en Réseaux et Services from Telecom SudParis, Evry, France, in 2010, both in networks and telecoms. Since June 2015 he has been with The Department of Electrical Engineering at Ecole Mohammadia d'Ingénieurs as a PhD student. His research interests include network design, array processing, adaptative algorithms, statistics and machine learning.